



## Research Article

# How Useful can be CT Scan in the Differential Diagnosis of Pneumonia in Immunocompromised Children? The Experience at a Tertiary Care Pediatric Center

Chiara Russo<sup>1</sup>, Francesca Rizzo<sup>2</sup>, Virginia Sambuceti<sup>3</sup>, Lorenzo Anfigeno<sup>3</sup>, Maria Grazia Calevo<sup>4</sup>, Carlo Dufour<sup>5</sup>, Gianluca Dell'Orso<sup>5</sup>, Luca Arcuri<sup>5</sup>, Maura Faraci<sup>5</sup>, Elio Castagnola<sup>6\*</sup>, Maria Beatrice Damasio<sup>2</sup>

<sup>1</sup>Department of Neurosciences, rehabilitation, ophthalmology, genetics and maternal and child sciences, University of Genova, Italy

<sup>2</sup>IRCCS Istituto Giannina Gaslini, Department of Radiology, Genova, Italy

<sup>3</sup>IRCCS Ospedale Policlinico San Martino, Genova, Italy

<sup>4</sup>IRCCS Istituto Giannina Gaslini, Epidemiology and Biostatistics Unit, Scientific Direction, Genova, Italy

<sup>5</sup>IRCCS Istituto Giannina Gaslini, Hematology Unit, Genova, Italy

<sup>6</sup>IRCCS Istituto Giannina Gaslini, Department of Infectious Diseases, Genova, Italy

\*Corresponding author: Elio Castagnola, IRCCS Istituto Giannina Gaslini, Department of Infectious Diseases, Genova, Italy.

**Citation:** Russo C, Rizzo F, Sambuceti V, Anfigeno L, Calevo MG, et al., (2023) How Useful can be CT Scan in the Differential Diagnosis of Pneumonia in Immunocompromised Children? The Experience at a Tertiary Care Pediatric Center. Infect Dis Diag Treat 7: 243. DOI: 10.29011/2577-1515.100243

**Received Date:** 22 November 2023; **Accepted Date:** 27 November 2023; **Published Date:** 30 November 2023

### Abstract

**Background and Objective:** Identifying radiological findings evocative of pneumonia etiology in hematologic-pediatric patients is challenging, mainly due to the non-specificity of CT findings in this population. **Materials and Methods:** This is a retrospective study conducted in a tertiary care pediatric hospital. All hematological patients admitted from 02/01/2009 to 12/31/2021 with a chest CT-scan performed and an etiological diagnosis of pneumonia were included; we excluded pneumonia due to *Pneumocystis jirovecii*. Pneumonia etiological diagnosis was made by clinicians based on clinical, microbiological and radiological findings (according to guidelines) and was defined as “definite diagnosis”. The primary aim was to identify radiological findings suggestive alone of specific pneumonia etiology, secondary aims were agreement among “radiological” and “definite diagnosis”, and intra and inter-observer agreement. So, two radiologists (one Senior and one Junior), blinded to patient’s characteristics and “definite diagnosis”, performed two readings of CT-scans of included patients; for each reading, they hypothesized a “radiological diagnosis”. To reach the primary aim a sub-analysis of the “radiological diagnosis” with the highest agreement with “definite diagnosis” was performed. **Results:** Twenty-four CT scans from 23 hematological patients were analyzed. Pneumonia’s “definitive diagnosis” was fungal and bacterial in 16 and 8 cases, respectively; no definite diagnosis of viral pneumonia was identified in the period of study. Senior “radiological diagnosis” derived from the first reading (S1) was the one with the best agreement with “definite diagnosis” (83.3%). The sub-analysis of S1 suggested that no radiological findings were indicative alone of specific infectious etiology. Intra-observer agreement was higher comparing J1 vs. J2 than S1 vs. S2. Inter-observer agreement was slight. **Conclusions:** Our study confirms the non-specificity of CT-scan findings alone in children with hematologic diseases. However, senior expertise allowed us to achieve the correct radiological diagnosis (compared to “definite diagnosis”) in 83% of CT-readings. We believe it’s essential to teach the knowledge to the youngest, as the cooperation between infectious disease and radiologist specialists.

## Introduction

Etiological diagnosis of pulmonary infections in pediatric patients with hematologic malignancies or undergoing hematopoietic stem cell transplantation (HM-HSCT) can be challenging. According to guidelines, radiological findings, mostly identified at Computed Tomography (CT) scan, are required for diagnosis of invasive fungal disease with varying degrees of certainty [1,2], but they could be useful to suggest also a bacterial or viral etiology [3]. CT scans have been demonstrated to be useful for early detection and follow-up (repeating imaging) of pulmonary invasive fungal disease (IFD), with important correlations with patients' outcomes [4,5]. However, even if CT scans might have a great performance in the radiological identification of pneumonia in immunocompromised patients [6] and some findings could lead to a specific etiological diagnosis (e.g., halo sign and air crescent sign, suggesting IFD due to molds [7]), in most cases pulmonary lesions detected by CT scan are not specific in children [8-10].

Recently, CT pulmonary angiogram has been demonstrated useful in adults in identifying vessel occlusion sign (VOS), a radiological finding potentially helpful in the diagnosis of angio-invasive pulmonary aspergillosis [11-14]. Other studies, instead, identified segmental consolidation as more specific of bacterial pneumonia [15].

In pediatrics, despite the utility of CT scan in immunocompromised patients, there could be concerns because of the radiation exposure [16,17]. To overcome this issue, ultra-low doses CT scan was introduced in the last years, maintaining a good diagnostic performance [18]. Furthermore, as for the possible risk of renal failure, a recent study demonstrated a low rate of acute kidney injury among pediatric population when contrast medium was used [19].

In this retrospective single-center study, we evaluated the role of CT scan in helping in etiological differential diagnosis of pneumonia in HM-HSCT children.

## Patients and Methods

IRCCS Istituto Giannina Gaslini (IGG), Genoa (Italy), is a tertiary care children's hospital serving a region of 1.5 million inhabitants in the North-West of Italy, with a catchment area extended to the whole nation and many European and foreign countries for highly specialized medical and surgical pediatric care.

We retrospectively selected HM-HSCT patients admitted to IGG from February 1<sup>st</sup>, 2009 to December 31<sup>st</sup>, 2021 with a chest CT scan performed and a defined infectious etiological diagnosis of pneumonia: fungal (according to EORTC-MSG criteria [2]), bacterial (in presence of lung infiltrate in a patient with bacteremia

due to non-common skin contaminants or isolation of significant pathogens from bronchoalveolar lavage) or viral. We excluded patients with a diagnosis of *pneumocystis* pneumonia.

To derive the infectious etiological diagnosis (i.e., "definite diagnosis"), two infectious diseases specialist's expert in infections in immunocompromised hosts (EC and CR) reviewed the clinical records; based on clinical, microbiological and radiological findings, they classified the pulmonary infections as bacterial, fungal or viral. "Definite diagnosis" was considered the gold standard diagnosis.

The CT scans of the selected patients were retrospectively evaluated by one senior and one young radiologist, blinded to the "definite diagnosis", who performed two separate readings of all CT scans and proposed a diagnosis based on only radiological findings (i.e., "radiological diagnosis"). To reduce the risk of outcome bias, the two readings made by the same radiologist were performed about 1 month apart, and the senior radiologist designated to CT reading was selected if a period greater than 5 years had passed from the initial CT report to the beginning of this study.

The following clinical data obtained from clinical records were recorded: age, sex, hematological disease, and type of bone marrow transplantation.

The primary aim of the study was to identify radiological findings that alone allow for differentiating fungal, bacterial and viral pneumonia in HM-HSCT patients.

Secondary aims were:

- to evaluate the "radiological" and "definite diagnosis" concordance
- to evaluate the "intra-radiologist concordance", that is the concordance in radiological findings interpretation in 2 serial readings performed by the senior and the junior radiologists, comparing senior first (S1) versus senior second (S2) reading and junior first (J1) versus junior second (J2) reading;
- to evaluate "inter-radiologist concordance", that is the concordance in radiological finding interpretations between senior and junior radiologists, comparing S1 vs. J1 and S2 vs. J2.

## Image Analysis

CT scans performed in HM-HSCT patients with an infectious etiological diagnosis of pneumonia were collected and anonymized. A Siemens Somatom 64 slices CT scanner was used; the same examination protocol was applied for all readings: volumetric thoracic scan, 3 mm MPR reconstruction with lung and mediastinal windowing was applied.

A MEDLINE search was performed, using the following terms: “CT scan hematological malignancy pulmonary infection”, “CT scan pulmonary aspergillosis stem cell transplantation”, “CT scan pulmonary aspergillosis hematopoietic stem cell transplantation”, “CT scan pulmonary aspergillosis bone marrow transplantation”, to identify CT scan findings helpful in defining infectious etiological diagnosis of pneumonia in HM-HSCT patients. A total of 22 studies were identified [11-15,18-34], 13 of them [4,11-15,19,21,24,35-38] specifically describing different radiological findings in pediatric patients with fungal, bacterial and viral pneumonia.

Based on these results, a CT scan reading table (Table 1) was created. See figure 1a, 1b, 2a, 2b, 3a, 3b, 4a, 4b, 5a, 5b for radiological signs examples. “Hypodense sign” (HyS) (Figure 1b, 2b, 5a) was defined as a central hypodensity in lung consolidation or nodule, corresponding to a central area of necrosis caused by vascular obstruction with secondary lung infarction and sequestration in angioinvasive pulmonary aspergillosis (IPA). It was firstly described by Horger et al in 43 immunocompromised patients undergone chest CT scan [39]. “Halo sign” (Figure 2a) was defined as ground-glass opacity surrounding a pulmonary nodule or mass; “air-crescent sign” (Figure 1a) as the presence of air in a crescent shape in a nodule or mass, and “reversed halo sign” as a focal rounded area of ground-glass opacity surrounded by a crescent or complete ring of consolidation.

Radiological finding	
Consolidation	Focal
	Multifocal
	Subsegmental
	Segmental
	Lobar
	Infarct shape
	With cavitation
	Halo sign
	Reversed halo sign
	Hypodense sign
Nodules	Single
	Multiples
	Small (≤ 10 mm)
	Big (> 10 mm)
	Both small and big

	Central
	Peripheral
	With cavitation
	Hypodense sign
	Halo sign
	Reversed halo sign
Tree in bud	
	Focal
	Multifocal
Cavern	
	Single
	Multiples
Pleural effusion	
	Monolateral
	Bilateral
Ground glass opacity	
	Focal
	Multifocal
	Central
	Peripheral
	Subsegmental
	Segmental
	Lobar
Crazy paving	
	Subsegmental
	Segmental
	Lobar
Vessel occlusion sign	
Hemorrhage	
Aneurysm/pseudoaneurysm	
Bronchiectasis	
Lymphadenomegaly	
	Monolateral
	Bilateral
	Single
	Multiple

**Table 1:** Radiological findings looked for by radiologists in CT scans.



**Figure 1:** Fungal infection.

Volumetric CT post contrast medium. MPR thin (3 mm) coronal reconstruction in a 10-years-old boy with acute T-cell leukemia, neutropenia, and persistent respiratory symptoms.

**Figure 1A:** Lung windowing: superior left lobe parenchymal consolidation (arrow) with air in a crescent shape within the nodule (air crescent sign). Small (<10mm) nodule with cavitation within subpleural region of inferior left lobe (short arrow).

**Figure 1B:** Mediastinal windowing: central hypodensity area (arrow) as result of a central area of necrosis (hypodense sign). Pleural effusion is evident in left lateral costophrenic recess (short arrow).

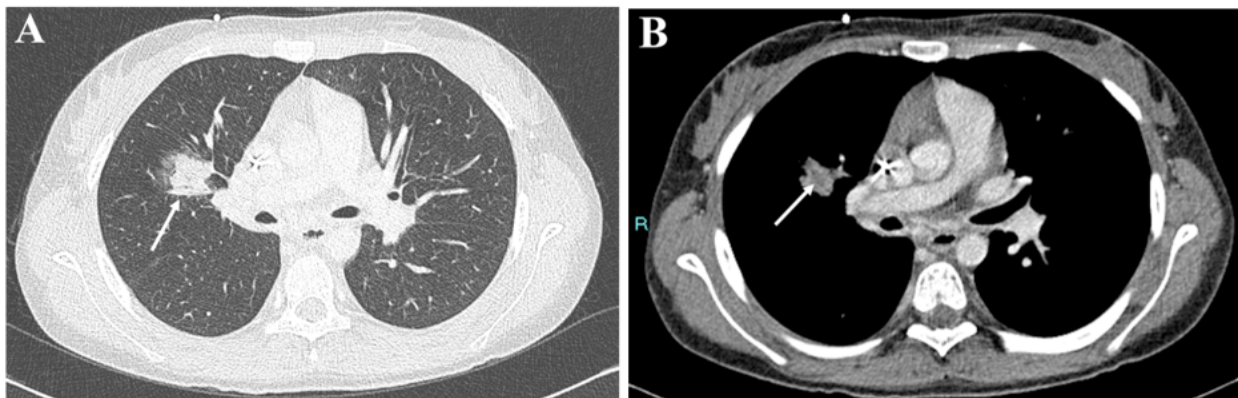


**Figure 2:** Aspergillosis.

Volumetric CT post contrast medium. MPR thin (3 mm) axial reconstruction in a 14-years-old girl with bone marrow aplasia, neutropenic, who underwent HSCT five months before pulmonary infection.

**Figure 2A** Lung windowing: focal subsegmental superior parahilar right consolidation (arrow). A halo of surrounding ground-glass opacity, halo sign, is evident around the lesion.

**Figure 2B** Mediastinal windowing: central hypodensity area (arrow) within the lesion as a result of a central area of necrosis (hypodense sign).



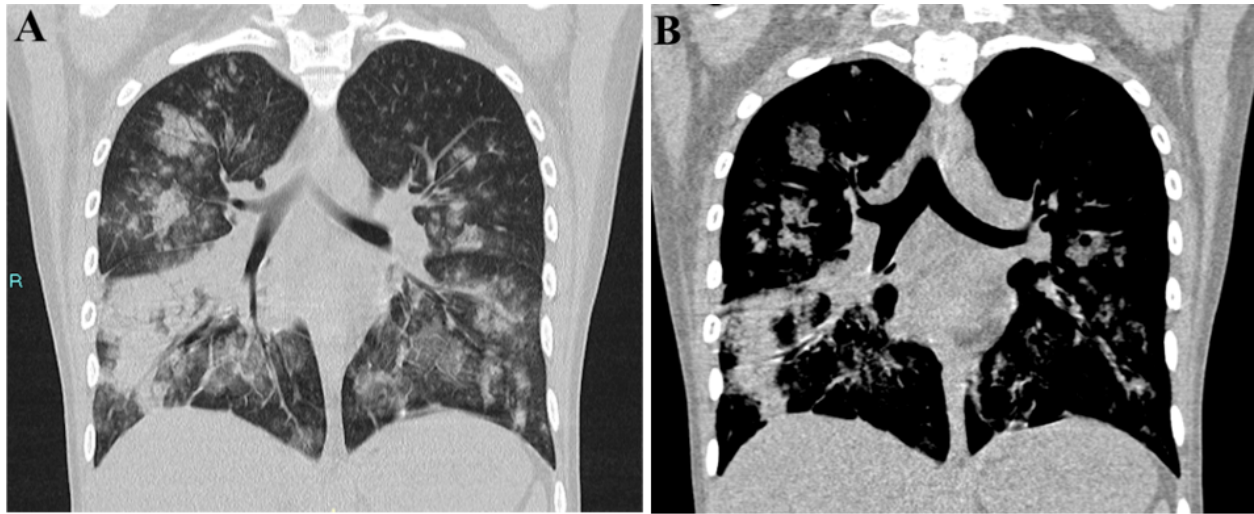


**Figure 3:** Bacterial pneumonia.

Volumetric CT post contrast medium. MPR thin (3 mm) coronal reconstruction in a 16-years-old girl with bone marrow hypoplasia, fever, respiratory symptoms, neutropenia.

**Figure 3A** Lung windowing: multiple diffuse bilateral areas of segmental and subsegmental consolidations involving central and peripheral portions of lungs. Also, diffuse bilateral areas of ground-glass opacities.

**Figure 3B** Mediastinal windowing: multiple diffuse bilateral areas of segmental and subsegmental consolidations involving central and peripheral portions of lungs. Also, diffuse bilateral areas of ground-glass opacities.

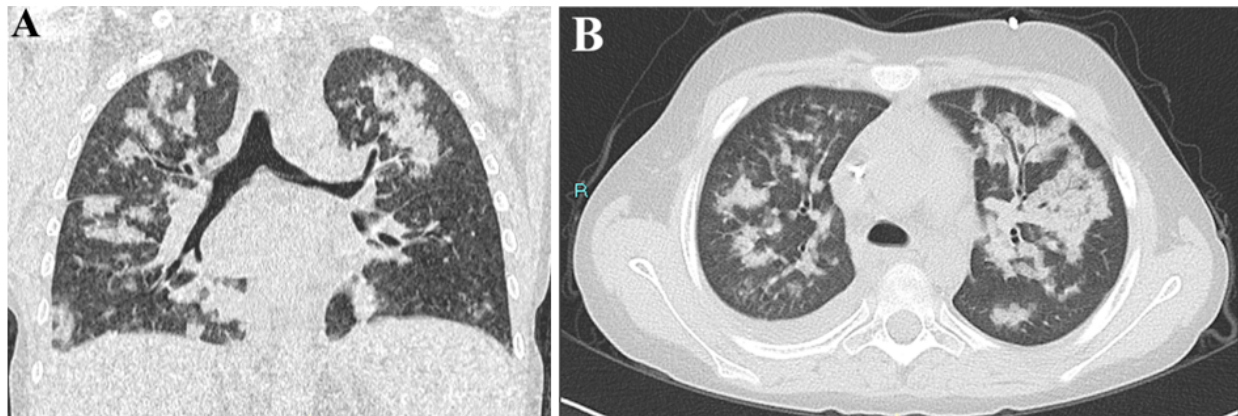


**Figure 4:** Bacterial pneumonia.

9-years -old boy with acute B-cell leukemia, fever, and desaturation, who underwent HSCT seven months before pulmonary infection.

**Figure 4A** Volumetric CT MPR thin (3 mm) coronal reconstruction. Lung windowing: bilateral areas of multifocal segmental/subsegmental consolidations at the level of the carina.

**Figure 4B** Volumetric CT MPR thin (3 mm) axial reconstruction. Mediastinal windowing: multifocal and multilobar distribution of the areas of consolidations with a prevalent central distribution at subcarinal level.

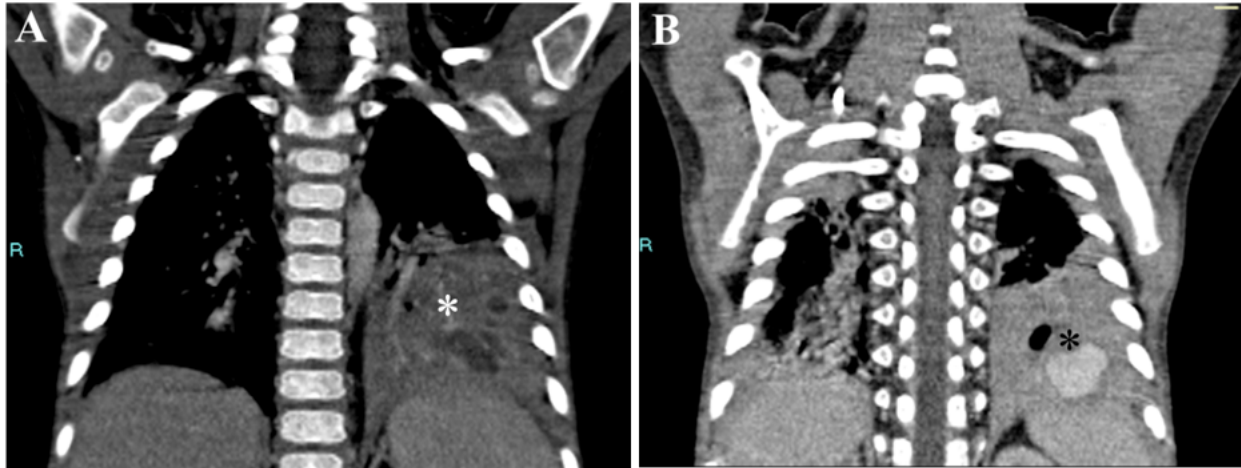


**Figure 5:** Bacterial pneumonia.

Volumetric CT MPR thin (3 mm) coronal reconstruction in a 19-months-old boy with acute myeloid leukemia, persistent fever, and respiratory symptoms.

**Figure 5A** Lung windowing: focal lobar consolidation (star) with a hypodense area within the lesion as a result of a central area of necrosis (hypodense sign).

**Figure 5B** Mediastinal windowing: focal hemorrhagic area within the lesion (star) associated with a cavitation area. Posterior contralateral basal dystelectatic consolidation is also evident.

Radiologists, one senior (BD, Pediatric Radiologist Physicians) and one junior (VS, Radiologist Resident), blinded for patients' clinical characteristics and the "definite diagnosis", performed two readings of every CT scan using the reading table. For each item in Table 1, the assessment options were "yes" when the radiologists identified the radiological sign, otherwise, they had to choose between "no" or "not assessable".

For each reading, radiologists had to hypothesize a diagnosis (bacterial, fungal, viral, or not identifiable infection), called "radiological diagnosis", based on imaging findings only. To derive the "radiological diagnosis" they relied on Table 2 [18]. At the end of the readings and diagnostic radiological hypothesis process, for each CT scan we had 4 "radiological diagnoses" (derived from first [S1] and second [S2] senior readings and from first [J1] and second [J2] junior readings) and one "definite diagnosis".

Diagnosis	CT finding
<b>Fungal pneumonia</b>	Nodules or patch areas of consolidation with a halo of surrounding ground-glass opacity cavitation or lung ball (late phase); or focal rounded area of ground-glass opacity surrounded by a crescent or complete ring of consolidation (reversed halo sign).
<b>Bacterial pneumonia</b>	Localized area of lobar, segmental, subsegmental or lobular consolidation, CT air-bronchogram, acinar nodules or tree-in-bud sign (so-called lobar or bronchopneumonia)
<b>Viral pneumonia</b>	Mosaic attenuation pattern (patchy areas of inhomogeneous lung attenuation caused by hyperventilation of alveoli distal to bronchiolar obstruction), patchy and poorly-defined areas of consolidation or bilateral patchy areas of GGO along bronchovascular bundles or along subpleural lungs in both lungs with random distribution, or bilateral lesions of centrilobular small nodule with short-branching pattern showing tree-in-bud signs

CT: computed tomography; GGO: ground-glass opacity

**Table 2:** Radiological appearance of different infectious diseases in immunocompromised hosts [18].

“Radiological diagnosis” was then compared with “definite diagnosis” and, based on the final diagnosis concordance, the “radiological diagnosis” with higher concordance with “definite diagnosis” was chosen and a sub-analysis of all radiological items included in the table was performed, trying to identify the single specific radiological finding that could allow to distinguish between different infectious pneumonia.

### Statistical analysis

Descriptive statistics were generated for the whole cohort and data were expressed as mean and standard deviation for continuous variables. Median value and range were calculated and reported, as were absolute or relative frequencies for categorical variables.

Non-parametric analysis (Mann–Whitney U-test) for continuous variables and Chi square or Fisher’s exact test for categorical variables were used to measure differences between the groups.

Intra-observer and inter-observer agreement was defined using Cohen’s kappa ( $\kappa$ ). Kappa values were interpreted using the following cut-offs: <0 poor, 0.00-0.20 slight, 0.21-0.40 fair, 0.41-0.60 moderate, 0.61-0.80 substantial, 0.81–1 almost perfect [40].

A *P* value less than 0.05 was considered statistically significant, and all values were based on two-tailed tests. Statistical analysis was performed using SPSS for Windows (SPSS Inc., Chicago, Illinois USA).

According to Italian legislation, the study did not need ethical approval since it was a purely observational retrospective study and therefore it was not possible to request informed consent for participation. In any case, consent to completely anonymous use of clinical data for research/epidemiological purposes is requested by the clinical routine at the time of admission/diagnostic procedure.

### Results

#### Patients

Overall, 24 pulmonary infections in 23 HM-HSCT patients, were included in the study: 16 (67%) with a “definite diagnosis” of invasive fungal disease (4 proven aspergillosis, 1 proven zygomycosis, 1 proven cryptococcosis, 8 probable aspergillosis, 2 possible aspergillosis), 8 (33%) of bacterial pneumonia. No patients with a “definite diagnosis” of viral pneumonia were identified. Intravenous radiocontrast was used in 16 (67%) cases. Thirteen patients were male (54.2%), the median age at the time of pulmonary infection was 12.29 years ranging between 0.44-20.34 years ( $10.79 \pm 5.96$  years). Table 3 reports on clinical characteristics of detected cases.

	<b>Total patients</b> N=24	<b>Bacterial diagnosis</b> N=8 (33.3%)	<b>Fungal diagnosis</b> N=16 (66.7%)	<b>Viral diagnosis</b> N=0 (0%)
	<b>N (%)</b>	<b>N (%)</b>	<b>N (%)</b>	<b>N (%)</b>
<b>Male</b>	13 (54.2)	4 (50.0)	9 (56.3)	0 (0)
<b>Bone marrow transplantation</b>	8 (33.3)	3 (37.5)	5 (31.3)	0 (0)
<b>Neutropenia at time of diagnosis</b>	13 (54.2)	3 (37.5)	10 (60.5)	0 (0)
<b>Acute lymphoid leukemia</b>	8 (33.3)	2 (25.0)	6 (37.5)	0 (0)
<b>Acute myeloid leukemia</b>	4 (16.7)	2 (25.0)	2 (12.5)	0 (0)
<b>Other hematological disease</b>	12 (50.0)	4 (50.0)	8 (50.0)	0 (0)

**Table 3:** Patient’s characteristics.

### “Radiological diagnosis” and “definite diagnosis” concordance

The frequency of different etiological diagnoses based on “radiological diagnosis” and “definite diagnosis” is reported in Table 4. In 2 cases the initial CT scan report was expressed by the senior radiologist, 5 and 7 years before this study was started.

	Etiological diagnosis of the 24 CT scans			
	Bacterial, n (%)	Fungal, n (%)	Viral, n (%)	Non-specific/negative, n (%)
<b>S1 radiological diagnosis</b>	7 (29.2)	13 (54.2)	0 (0.0)	4 (16.7)
<b>S2 radiological diagnosis</b>	8 (33.3)	11 (45.8)	0 (0.0)	5 (20.8)
<b>J1 radiological diagnosis</b>	11 (45.8)	7 (29.2)	5 (20.8)	1 (4.2)
<b>J2 radiological diagnosis</b>	10 (41.7)	9 (37.5)	4 (16.7)	1 (4.2)
<b>Definite diagnosis</b>	8 (33.3)	16 (66.7)	0 (0.0)	0 (0.0)

Abbreviations: S1: senior first “radiological diagnosis”; S2: senior second “radiological diagnosis”; J1: junior first “radiological diagnosis”; J2: junior second “radiological diagnosis”.

**Table 4:** Frequency of different etiological diagnosis according to the four “radiological diagnosis” and “definite diagnosis”.

Senior radiologist classified the CT scans as non-specific/negative in 4 cases in the first and in 5 cases in the second reading; no CT scan was suggestive of viral pneumonia according to senior radiologist’s opinion.

Junior radiologist classified 5 and 4 CT scans in the first and second readings, respectively, as indicative of viral pneumonia. In only 1 case for each CT scan reading junior radiologist classified the imaging as non-specific/negative.

The comparison of “radiological diagnosis” (S1, S2, J1, J2) with “definite diagnosis” showed different grades of agreement with “definite diagnosis”; the first reading made by the senior radiologist (S1) was the one with the best agreement (moderate agreement) with “definite diagnosis” (Kappa 0.69, 95%CI 0.45;0.93. Agreement 83.3%,). Looking at other “radiological diagnoses” and agreement with “definite diagnosis”, S2 had 75% (Kappa 0.57, 95%CI 0.32;0.82), J1 37.5% (Kappa 0.04, 95%CI -0.17;0.26) and J2 45.8% (Kappa 0.11, 95%CI -0.13;0.36) of agreement, respectively (Table 5).

Radiological vs. definite diagnosis	Intra-Observer		Inter-Observer	
	Kappa (95% CI) (Agreement)	Kappa (95% CI) (Agreement)	Kappa (95% CI) (Agreement)	Kappa (95% CI) (Agreement)
<b>S1 vs. Definite Diagnosis</b>	0.69 (0.45;0.93) (83.3%)	<b>S1 vs. S2</b> 0.73 (0.49;0.97) (83.3%)	<b>S1 vs. J1</b>	0.11 (-0.13;0.35) (37.5%)
<b>S2 vs. Definite Diagnosis</b>	0.57 (0.32;0.82) (75%)	<b>J1 vs. J2</b> 0.81 (0.61;1.0) (87.5%)	<b>S2 vs. J2</b>	0.20 (-0.06;0.46) (45.8%)
<b>J1 vs. Definite Diagnosis</b>	0.04 (-0.17;0.26) (37.5%)			
<b>J2 vs. Definite Diagnosis</b>	0.11 (-0.13;0.36) (45.8%)			

**Table 5:** Radiological diagnosis and concordance among different readings and definite diagnosis.

### Intra-radiologist’ concordance

We studied concordance among “radiological diagnosis”, comparing 1<sup>st</sup> and 2<sup>nd</sup> senior (S1 vs. S2) and junior (J1 vs. J2) CT-scan readings. The intra-observer agreement between S1 and S2 was substantial (Kappa 0.73, 95%CI 0.49;0.97. Agreement 83.3%), and was almost perfect between J1 vs. J2 (Kappa 0.81, 95%CI 0.61;1.0. Agreement 87.5%), Table 5. In Table 6 we reported intra-observer (S1 vs. S2; J1 vs. J2) agreement for all the main radiological findings identified by radiologist in first and second CT-scan readings. Even if J1 vs. J2 “radiological diagnosis” had better agreement than S1 vs. S2 “radiological diagnosis”, looking at the individual radiological findings, agreement was higher comparing S1 vs. S2 CT scan readings than J1 vs. J2, except for vessel occlusion sign and lymphadenomegaly.



RADIOLOGICAL FINDINGS		Consolidation	Nodules	Tree in bud	Cavern	Crazy paving	Vessel occlusion sign	Hemorrhage	Aneurysm	Bronchiectasis	Lymphadenomegaly
		Kappa (95%CI) (Agreement)	Kappa (95%CI) (Agreement)	Kappa (95%CI) (Agreement)	Kappa (95%CI) (Agreement)	Kappa (95%CI) (Agreement)	Kappa (95%CI) (Agreement)	Kappa (95%CI) (Agreement)	Kappa (95%CI) (Agreement)	Kappa (95%CI) (Agreement)	Kappa (95%CI) (Agreement)
<i>Intra-radiologist' concordance</i>	<b>S1 vs. S2</b>	0.78 (0.49;1.0) (91.7%)	0.75 (0.49;1.0) (87.5%)	0.75 (0.43;1.0) (91.7%)	1 (1;1) (100%)	0.65 (0.02;1.0) (95.8%)	0.65 (0.31;0.99) (87.5%)	0.08 (-0.36;0.52) (70.8%)	0.89 (0.69;1.0) (95.8%)	0.62 (0.16;1.0) (91.7%)	0.58 (0.30;0.85) (75.0%)
	<b>J1 vs. J2</b>	0.32 (-0.14;0.78) (79.2%)	0.50 (0.17;0.83) (75%)	0.78 (0.49;1.0) (91.7%)	0.50 (0.01;0.98) (87.5%)	0 (N.E.) * (91.7%)	1 (1 ;1) (100%)	N.E. * (100%)	N.E. * (100%)	0.43 (0.11;0.76) (70.8%)	0.68 (0.40;0.95) (83.3%)
<i>Inter-radiologist' concordance</i>	<b>S1 vs. J1</b>	0.50 (0.08;0.91) (83.3%)	0.67 (0.37;0.96) (83.3%)	0.56 (0.17;0.94) (83.3%)	0.47 (-0.13;1.0) (91.7%)	0 (N.E.) * (95.8%)	-0.08 (-0.08 ;0.02) (79.2%)	0 (N.E.) * (79.2%)	0 (N.E.) * (75%)	-0.07 (0.41;0.27) (58.3%)	0.45 (0.14;0.76) (70.8%)
	<b>S2 vs. J2</b>	0.65 (0.28;1.0) (87.5%)	0.55 (0.20;0.89) (79.2%)	0.75 (0.43;1.0) (91.7%)	0.36 (-0.16;0.88) (87.5%)	0 (-0.18;0) (83.3%)	0 (0;0.03) (66.7%)	0 (N.E.) * (83.3%)	0 (N.E.) * (70.8%)	0.14 (-0.04;0.33) (54.2%)	0.52 (0.25;0.79) (70.8%)

Abbreviations: S1: senior first "radiological diagnosis"; S2: senior second "radiological diagnosis"; J1: junior first "radiological diagnosis"; J2: junior second "radiological diagnosis".  
\*Not Evaluable

**Table 6:** Intra (S1 vs. S2; J1 vs. J2) and inter (S1 vs. J1; S2 vs. J2) radiologist concordance for each main radiological finding used by radiologists for CT-scan readings.

**Inter-radiologists' concordance**

We found a slight concordance comparing both S1 vs. J1 "radiological diagnosis" (Kappa 0.11, 95%CI -0.13;0.35. Agreement 37.5%) and S2 vs. J2 "radiological diagnosis" (Kappa 0.20, 95%CI -0.06;0.46. Agreement 45.8%), Table 5. Looking at concordance between the main individual radiological findings (Table 7), we did not find differences between S1 vs. J1 and S2 vs. J2 CT-scan readings, except for "vessel occlusion sign", for which concordance was higher comparing S1 vs. J1 than S2 vs. J2.

	Fungal pneumonia	Bacterial pneumonia	P value
Total	N = 16	N = 8	
<b>Radiological finding</b>			
Consolidation	12 (75)	6 (75)	1
Focal	8 (66.7)	5 (50)	0.63
Multifocal	2 (16.7)	3 (50)	0.27
Subsegmental	3 (25)	1 (16.7)	1
Segmental	8 (66.7)	3 (50)	0.63
Lobar	2 (16.7)	2 (33.3)	0.57
Infarct shape	0	0	-
With cavitation	2 (16.7)	1 (16.7)	1
Halo sign	5 (41.7)	1 (16.7)	0.31
Reversed halo sign	1 (8.3)	1 (16.7)	1
Hypodense sign	3 (25)	1 (16.7)	0.83
Nodules	8 (50)	4 (50)	1
Single	5 (62.5)	1 (25)	0.54
Multiple	3 (37.5)	3 (75)	0.54
Small (□ 10 mm)	7 (87.5)	3 (75)	1
Big (> 10 mm)	2 (25)	1 (25)	1
Both small and big	1 (12.5)	0	1
Central	6 (75)	3 (75)	1
Peripheral	5 (62.5)	3 (75)	1
With cavitation	4 (50)	0	0.21
Hypodense sign	1 (12.5)	0	1
Halo sign	1 (12.5)	1 (25)	1
Reversed halo sign	0	0	-
Tree in bud	4 (25)	2 (25)	1
Focal	3 (75)	0	0.40
Multifocal	1 (25)	2 (100)	0.40
Cavern	0	1 (12.5)	0.33
Single	-	1 (100)	-
Multiples	-	-	-
Pleural effusion	1 (6.2)	2 (25)	0.25
Monolateral	1 (100)	2 (100)	-
Bilateral	-	-	-
Ground glass opacity	7 (43.8)	6 (75)	0.21
Focal	4 (57.1)	2 (33.3)	0.59
Multifocal	2 (28.6)	4 (66.7)	0.29
Central	0	2 (33.3)	0.19
Peripheral	7 (100)	3 (50)	<b>0.07</b>
Subsegmental	4 (57.1)	2 (33.3)	0.59
Segmental	2 (28.6)	3 (50)	0.59
Lobar	0	1 (16.7)	0.46
Crazy paving	0	1 (12.5)	0.33
Subsegmental	-	1 (100)	-
Segmental	-	1 (100)	-
Lobar	-	1 (100)	-
Vessel occlusion sign	2 (12.5)	2 (25)	0.58
Hemorrhage	0	1 (12.5)	0.31
Aneurysm/pseudoaneurysm	4 (25)	2 (25)	1
Bronchiectasis	1 (6.2)	3 (37.5)	<b>0.09</b>
Lymphadenomegaly	10 (62.5)	4 (50)	0.26
Monolateral	6 (60)	2 (50)	1
Bilateral	4 (40)	2 (50)	1
Single	3 (30)	1 (25)	1
Multiple	7 (70)	3 (75)	1
Mean age ± SD	10.84±6.29	10.69±5.66	0.83
Median age (min; max)	12.93 (0.44; 20.34)	11.40 (1.62; 18.58)	

**Table 7:** Frequency of different radiological findings at 1st reading made by senior radiologist (S1) in "definite diagnosis" of bacterial and fungal pneumonia in children with hematologic malignancies or undergoing hematopoietic stem cell transplantation.

**CT scan main findings**

Since the primary outcome was to identify radiological findings useful in defining the infectious etiology of pneumonia in HM-HSCT population, we chose the “radiological diagnosis” with the higher agreement with “definite diagnosis” (S1) for this evaluation, subsequently analyzing the frequency of different radiological findings in bacterial and fungal pneumonia, as defined by the radiologist in S1 “radiological diagnosis” (Table 7).

Almost none of the radiological findings was specific for fungal or bacterial pneumonia (Table 6). Particularly, consolidation was present in the same proportion in patients with radiological diagnosis of bacterial and fungal pneumonia, but in bacterial pneumonia it was more frequently multifocal and lobar, while in fungal pneumonia focal, even if statistical significance was not reached. Halo sign was found more frequently in fungal pneumonia, while nodules were represented in 50% of both bacterial and fungal pneumonia, but they resulted more frequently single and cavitated in fungal pneumonia, multiple in bacterial pneumonia. Ground glass opacities were multifocal and central in most cases of bacterial pneumonia, peripheral in fungal pneumonia. Presence of vessel occlusion sign and aneurysm/pseudoaneurysm were not useful in differential diagnosis between bacterial and fungal pneumonia.

## Discussion

In the present study, we evaluated the contribution of CT scan in the differential diagnosis of pneumonia in HM-HSCT children with radiologists blinded to clinical and microbiological data. In this condition, the 1<sup>st</sup> “radiological diagnosis” made by a senior radiologist had the best concordance with the “definite diagnosis”, but none of the radiological findings were significantly associated with diagnosis of bacterial or fungal pneumonia (Table 7), confirming the lower specificity of imaging in pediatrics, compared with adults [41]. For example, halo sign, that in adults is considered highly specific for invasive pulmonary aspergillosis, in our cohort was identified not only in 41.7% of CT scans of patients with a diagnosis of IFD, but also in 16.7% of those with a diagnosis of bacterial pneumonia. Moreover, cavitation was observed in the presence of both infections, but in this case the presence or absence of neutropenia, a “clinical” datum, represented the driver for the definite diagnosis, with cavitory lesions in neutropenic patients not related with invasive mycosis [42]. Finally, vessel occlusion that has been suggested as a sign of mold pneumonia in adults [12-14,21] was observed only in 12.5% of children with fungal pneumonia and 25% of those with bacterial infection.

Another interesting observation was that radiologists are consistent with their own readings, with intra-radiologist concordance higher for junior radiologist (J1 vs. J2 “radiological diagnosis”) than between senior (S1 vs. S2). A possible explanation for the higher intra-observer concordance in J1 vs. J2 is that

junior radiologists tend to be more adherent to scientific and academic descriptions of radiological signs, which are also more reproducible, while senior radiologists rely not only on academic definitions, but also on personal experience. These might also explain the substantial agreement between senior “radiological diagnosis” and “definite diagnosis”, which was lower comparing junior “radiological diagnosis” to “definite diagnosis”, and consequently the low inter-observer agreement. Looking at Table 3, we can also hypothesize that senior radiologists were not only more confident in identifying fungal and bacterial radiological findings (compared to “definite diagnosis”) but were also more confident in saying that CT scans were non-specific in some cases. On the contrary, junior radiologist was probably less confident in defining the imaging as non-specific, classifying 5 and 4 CT scans in J1 and J2 readings, respectively, as viral.

Intriguingly, the concordance between 1<sup>st</sup> senior radiologist diagnosis and “definite diagnosis” was substantial (Kappa 0.69, 95%CI 0.45;0.93. Agreement 83.3%), while the 2<sup>nd</sup> had a lower agreement, suggesting that “a second look” could have entered doubts even in senior radiologist if not sustained by clinical, laboratory and microbiological data.

The major limitation of our study is the small sample size (23 patients over a period of 12 years), which could be explained by the careful application of antifungal prophylaxis protocol. Due to this issue, it is difficult to identify radiological findings able to diversify with statistical significance between bacterial or fungal pneumonia. However, a senior radiologist, who has expertise in pediatric and immunocompromised patients, was able to draw up a “radiological diagnosis” concord with “definite diagnosis” in 83.3% of cases, highlighting a good radiological diagnostic performance. Moreover, the blinded readings of CT scans made by two groups of radiologists increase the importance of our findings and at the same time underlines the need for cooperation between radiologists and clinicians’ experts in the management of infections in HM-HSCT pediatric patients. Indeed, the low specificity of radiological findings in this specific population makes it necessary to combine imaging with clinical, laboratory and microbiological data [24,37] to come to a correct diagnosis.

In conclusion, our study confirms that CT scan findings in pneumonia in HM-HSCT children are frequently not specific. What is in our opinion the most important observation is that CT findings must be interpreted in the light of clinical, laboratory and microbiological data, meaning the need of strict cooperation between radiologists and clinicians taking care of infections in immunocompromised children. This cooperation among different specialists must be extended to teaching younger medical doctors to provide the best care, especially in complex patient populations such as HM-HSCT children.

**Conflict of Interest Disclosures (includes financial disclosures):**

The authors have no conflict of interest relevant to this article to disclose.

**Funding/Support:** The study was partially supported by a grant from the “Ministero della salute ricerca corrente”.

**References**

- Alexander BD, Lamoth F, Heussel CP, Prokop CS, Desai SR, et al., (2021) Guidance on Imaging for Invasive Pulmonary Aspergillosis and Mucormycosis: From the Imaging Working Group for the Revision and Update of the Consensus Definitions of Fungal Disease from the EORTC/MSGERC. *Clin Infect Dis* 72: S79-S88.
- Donnelly JP, Chen SC, Kauffman CA, Steinbach WJ, Baddley JW, et al., (2020) Revision and Update of the Consensus Definitions of Invasive Fungal Disease From the European Organization for Research and Treatment of Cancer and the Mycoses Study Group Education and Research Consortium. *Clin Infect Dis* 71:1367-1376.
- Winer-Muram HT, Arheart KL, Jennings SG, Rubin SA, Kauffman WM, et al., (1997) Pulmonary complications in children with hematologic malignancies: accuracy of diagnosis with chest radiography and CT. *Radiology* 204:643-649.
- Caillot D, Casasnovas O, Bernard A, Couaillier JF, Durand C, et al., (1997) Improved management of invasive pulmonary aspergillosis in neutropenic patients using early thoracic computed tomographic scan and surgery. *J Clin Oncol* 15:139-147.
- Caillot D, Couaillier JF, Bernard A, Casasnovas O, Denning DW, et al., (2001) Increasing volume and changing characteristics of invasive pulmonary aspergillosis on sequential thoracic computed tomography scans in patients with neutropenia. *J Clin Oncol* 19:253-259.
- Taccone A, Occhi M, Garaventa A, Manfredini L, Viscoli C (1993) CT of invasive pulmonary aspergillosis in children with cancer. *Pediatr Radiol* 23:177-180.
- Toma P, Bertaina A, Castagnola E, Colafati GS, D'Andrea ML, et al., (2016) Fungal infections of the lung in children. *Pediatr Radiol* 46:1856-1865.
- Burgos A, Zaoutis TE, Dvorak CC, Hoffman JA, Knapp KM, et al., (2008) Pediatric invasive aspergillosis: a multicenter retrospective analysis of 139 contemporary cases. *Pediatrics* 121: e1286-1294.
- Thomas KE, Owens CM, Veys PA, Novelli V, Costoli V (2003) The radiological spectrum of invasive aspergillosis in children: a 10-year review. *Pediatr Radiol* 33:453-460.
- Lewis RE, Stanzani M, Morana G, Sassi C (2023) Radiology-based diagnosis of fungal pulmonary infections in high-risk hematology patients: are we making progress? *Curr Opin Infect Dis* 36:250-256.
- Herbrecht R, Roedlich MN (2012) Earlier diagnosis of angioinvasive pulmonary mold disease: is computed tomography pulmonary angiography a new step? *Clin Infect Dis* 54:617-620.
- Sassi C, Stanzani M, Lewis RE, Facchini G, Bazzocchi A, et al., (2018) The utility of contrast-enhanced hypodense sign for the diagnosis of pulmonary invasive mould disease in patients with haematological malignancies. *Br J Radiol* 91:20170220.
- Stanzani M, Battista G, Sassi C, Lewis RE, Tolomelli G, et al., (2012) Computed tomographic pulmonary angiography for diagnosis of invasive mold diseases in patients with hematological malignancies. *Clin Infect Dis* 54:610-616.
- Stanzani M, Sassi C, Lewis RE, Tolomelli G, Bazzocchi A, et al., (2015) High resolution computed tomography angiography improves the radiographic diagnosis of invasive mold disease in patients with hematological malignancies. *Clin Infect Dis* 60:1603-1610.
- Chen W, Xiong X, Xie B, Ou Y, Hou W, et al., (2019) Pulmonary invasive fungal disease and bacterial pneumonia: a comparative study with high-resolution CT. *Am J Transl Res* 11:4542-4551.
- Brenner DJ, Hall EJ (2007) Computed tomography--an increasing source of radiation exposure. *N Engl J Med* 357:2277-2284.
- Pearce MS, Salotti JA, Little MP, McHugh K, Lee C, et al., (2012) Radiation exposure from CT scans in childhood and subsequent risk of leukaemia and brain tumours: a retrospective cohort study. *Lancet* 380:499-505.
- Kim HJ, Park SY, Lee HY, Lee KS, Shin KE, et al., (2014) Ultra-Low-Dose Chest CT in Patients with Neutropenic Fever and Hematologic Malignancy: Image Quality and Its Diagnostic Performance. *Cancer Res Treat* 46:393-402.
- Henzler C, Henzler T, Buchheidt D, Nance JW, Weis CA, et al., (2017) Diagnostic Performance of Contrast Enhanced Pulmonary Computed Tomography Angiography for the Detection of Angioinvasive Pulmonary Aspergillosis in Immunocompromised Patients. *Sci Rep* 7:4483.
- Porto L, You SJ, Attarbaschi A, Cario G, Döring M, et al., (2020) Invasive Mold Infection of the Central Nervous System in Immunocompromised Children. *J Fungi (Basel)* 6:226.
- Stanzani M, Sassi C, Lewis R, Sartor C, Rasetto G, et al., (2021) Early low-dose computed tomography with pulmonary angiography to improve the early diagnosis of invasive mould disease in patients with haematological malignancies: A pilot study. *J Infect* 83:371-380.
- Stanzani M, Sassi C, Battista G, Lewis RE (2019) Beyond biomarkers: How enhanced CT imaging can improve the diagnostic-driven management of invasive mould disease. *Med Mycol* 57:S274-S286.
- Wang JW, Yang FF, Zhang CY, Lin JZ, Wang HX, et al., (2021) Imaging Characteristics of Invasive Pulmonary Fungal Infection Secondary to Hematological Diseases and Comparison before and after Treatment. *J Healthc Eng* 2021:3736108.
- Wang X, Guo G, Cai R, He P, Zhang M (2019) Utility of serum galactomannan antigen testing combined with chest computed tomography for early diagnosis of invasive pulmonary aspergillosis in patients with hematological malignancies with febrile neutropenia after antifungal drug treatment. *J Int Med Res* 47:783-790.
- Burivong W, Sricharoen T, Thachang A, Soodchuen S, Maroongroge P, et al., (2021) Early Radiologic Diagnosis of Pulmonary Infection in Febrile Neutropenic Patients: A Comparison of Serial Chest Radiography and Single CT Chest. *Radiol Res Pract* 2021:8691363.
- Agrawal R, Yeldandi A, Savas H, Parekh ND, Lombardi PJ, et al., (2020) Pulmonary Mucormycosis: Risk Factors, Radiologic Findings, and Pathologic Correlation. *Radiographics* 40:656-666.
- Stemler J, Bruns C, Mellinghoff SC, Alakel N, Akan H, et al., (2020) Baseline Chest Computed Tomography as Standard of Care in High-Risk Hematology Patients. *J Fungi (Basel)* 6:36.

28. Bitterman R, Hardak E, Raines M, Stern A, Zuckerman T, et al., (2019) Baseline Chest Computed Tomography for Early Diagnosis of Invasive Pulmonary Aspergillosis in Hemato-oncological Patients: A Prospective Cohort Study. *Clin Infect Dis* 69:1805-1808.
29. Gerritsen MG, Willemink MJ, Pompe E, Bruggen T, Rhenen A, et al., (2017) Improving early diagnosis of pulmonary infections in patients with febrile neutropenia using low-dose chest computed tomography. *PLoS One* 12: e0172256.
30. Vehreschild JJ, Heussel CP, Groll AH, Vehreschild MJ, Silling G, et al., (2017) Serial assessment of pulmonary lesion volume by computed tomography allows survival prediction in invasive pulmonary aspergillosis. *Eur Radiol* 27:3275-3282.
31. Roques M, Chretien ML, Favennec C, Lafon I, Ferrant E, et al., (2016) Evolution of procalcitonin, C-reactive protein and fibrinogen levels in neutropenic leukaemia patients with invasive pulmonary aspergillosis or mucormycosis. *Mycoses* 59:383-390.
32. Sharma R, Singh C, Khadwal A, Prakash G, Malhotra P, et al., (2021) Role of pre-transplant chest high-resolution computed tomography and serum galactomannan index in predicting post-transplant invasive pulmonary aspergillosis in allogeneic hematopoietic cell transplant recipients. *Transpl Infect Dis* 23: e13632.
33. Ceasay MM, Desai SR, Cleverley J, Berry L, Smith M, et al., (2018) Pre-symptomatic (Baseline) computed tomography predicts invasive pulmonary aspergillosis in high-risk adult haemato-oncology patients. *Br J Haematol* 182:723-727.
34. El Boghdady Z, Oran B, Jiang Y, Rondon G, Champlin R, et al., (2017) Pretransplant chest computed tomography screening in asymptomatic patients with leukemia and myelodysplastic syndrome. *Bone Marrow Transplant* 52:476-479.
35. Casutt A, Couchepin J, Brunel AS, Lovis A, Bochud P-Y, et al., (2020) High prevalence of peribronchial focal lesions of airway invasive aspergillosis in hematological cancer patients with prolonged neutropenia. *Br J Radiol* 93:20190693.
36. Lin CY, Wang IT, Chang CC, Lee WC, Liu WL, et al., (2019) Comparison of Clinical Manifestation, Diagnosis, and Outcomes of Invasive Pulmonary Aspergillosis and Pulmonary Mucormycosis. *Microorganisms* 7:531.
37. Qiu KY, Liao XY, Huang K, Xu HG, Li Y, et al., (2019) The early diagnostic value of serum galactomannan antigen test combined with chest computed tomography for invasive pulmonary aspergillosis in pediatric patients after hematopoietic stem cell transplantation. *Clin Transplant* 33: e13641.
38. Zaleska-Dorobisz U, Olchowy C, Lasecki M, Sokołowska-Dąbek D, Pawluś A, et al., (2017) Low-dose computed tomography in assessment of pulmonary abnormalities in children with febrile neutropenia suffering from malignant diseases. *Adv Clin Exp Med* 26:695-701.
39. Horger M, Einsele H, Schumacher U, Wehrmann M, Hebart H, et al., (2005) Invasive pulmonary aspergillosis: frequency and meaning of the "hypodense sign" on unenhanced CT. *Br J Radiol* 78:697-703.
40. Landis JR, Koch GG (1977) The measurement of observer agreement for categorical data. *Biometrics* 33:159-174.
41. Lehrnbecher T, Hassler A, Groll AH, Bochennek K (2018) Diagnostic Approaches for Invasive Aspergillosis-Specific Considerations in the Pediatric Population. *Front Microbiol* 9:518.
42. Castagnola E, Viscoli C, Mikulska M (2015) Prophylaxis and empirical therapy of infections in cancer patients. *Mandell, Douglas and Bennett Principles and Practice of Infectious Diseases* 3395–3413.e2.